Article

New Mononuclear Cu(II) Complexes and 1D Chains with 4-Amino-4*H*-1,2,4-triazole

Marinela M. Dîrtu [1], Yves Boland [1], Damien Gillard [1], Bernard Tinant [1], Koen Robeyns [1], Damir A. Safin [1], Eamonn Devlin [2], Yiannis Sanakis [2] and Yann Garcia [1,*]

[1] Institute of Condensed Matter and Nanosciences, Université Catholique de Louvain, Molecules, Solids and Reactivity (IMCN/MOST), Place L. Pasteur, 1, Louvain-la-Neuve 1348, Belgium; E-Mails: marinela.dirtu@uclouvain.be (M.M.D.); boland@chim.ucl.ac.be (Y.B.); damien.gillard@hotmail.com (D.G.); bernard.tinant@uclouvain.be (B.T.); koen.robeyns@uclouvain.be (K.R.); damir.safin@uclouvain.be (D.A.S.)

[2] Institute for Advanced Materials, Physicochemical Processes, Nanotechnology & Microsystems, NCSR Demokritos, Athens 15310, Greece; E-Mails: edevlin@ims.demokritos.gr (E.D.); sanakis@ims.demokritos.gr (Y.S.)

* Author to whom correspondence should be addressed; E-Mail: yann.garcia@uclouvain.be; Tel.: +32-10-47-28-26; Fax: +32-10-47-23-30.

Abstract: The crystal structures of two mononuclear Cu(II) NH_2trz complexes $[Cu(NH_2trz)_4(H_2O)](AsF_6)_2$ (**I**) and $[Cu(NH_2trz)_4(H_2O)](PF_6)_2$ (**II**) as well as two coordination polymers $[Cu(\mu_2-NH_2trz)_2Cl]Cl \cdot H_2O$ (**III**) and $[Cu(\mu_2-NH_2trz)_2Cl](SiF_6)_{0.5} \cdot 1.5H_2O$ (**IV**) are presented. Cationic 1D chains with bridging bis-monodentate μ_2-coordinated NH_2trz and bridging μ_2-coordinated chloride ligands are present in **III** and **IV**. In these coordination polymers, the Cu(II) ions are strongly antiferromagnetically coupled with $J = -128.4$ cm^{-1} for **III** and $J = -143$ cm^{-1} for **IV** ($H = -J\Sigma S_i S_{i+1}$), due to the nature of the bridges between spin centers. Inter-chain interactions present in the crystal structures were taken into consideration, as well as *g* factors, which were determined experimentally, for the quantitative modeling of their magnetic properties.

Keywords: coordination polymers; copper; 1,2,4-triazole; magnetic properties; crystal engineering

1. Introduction

There is constant interest in 1,2,4-triazoles and their derivatives, which are known as useful drugs thanks to their outstanding biological activities being used as, antifungal agents [1], plant protection fungicides [2], *etc*. On the other hand, 1,2,4-triazoles are also synthesized for other purposes, for instance in coordination chemistry as metal-azolate frameworks [3], or azole coordination polymers [4,5]. A variety of coordination networks can be designed thanks to the various coordination modes of 1,2,4-triazole-containing building blocks [4]. In particular, numerous oligonuclear and polymeric Cu(II) complexes have been reported with 4-amino-4*H*-1,2,4-triazole (NH_2trz) [6–17], presumably because it contains a primary $-NH_2$ group, which might be further used to functionalize the obtained products. In particular, a few examples of 1D chains were proposed as structural models of the corresponding Fe(II) complexes, which are known to present exceptional spin transition behavior, sometimes occurring around room temperature [18–20]. This includes [Cu(μ_2-NH_2trz)$_3$](BF_4)$_2 \cdot H_2O$ [21], [Cu(μ_2-NH_2trz)$_3$](BF_4)(SiF_6)$_{0.5} \cdot 2H_2O$ [21], [Cu(μ_2-NH_2trz)$_3$]$SiF_6 \cdot H_2O$ [21], [Cu(μ_2-NH_2trz)$_3$](NO_3)$_2 \cdot H_2O$ [18] and [Cu(μ_2-NH_2trz)$_3$]$ZrF_6 \cdot 2H_2O$ [22], which all exhibit a polymeric structure where Cu(II) atoms are linked in a 1D chain by the bridging bis-monodentate nitrogen atoms of the 1,2,4-triazole cycles. Interestingly, only two mononuclear Cu(II) NH_2trz complexes [23,24] are known. Following our continuing interest on the magnetic properties of these systems, we report on the synthesis and crystal structures of two new mononuclear Cu(II) complexes [Cu(NH_2trz)$_4$(H_2O)](AsF_6)$_2$ (**I**) and [Cu(NH_2trz)$_4$(H_2O)](PF_6)$_2$ (**II**). We also present the crystal structures and magnetic properties of two 1D chains [Cu(μ_2-NH_2trz)$_2$Cl]Cl$\cdot H_2O$ (**III**) and [Cu(μ_2-NH_2trz)$_2$Cl](SiF_6)$_{0.5} \cdot 1.5H_2O$ (**IV**) whose magnetic properties were studied quantitatively. We also detail the synthesis of a new bis-triazole molecule: *N*,*N'*-bis-(1,2,4-triazole-4-yl)formamidine hydrochloride (**L·HCl**) and describe its crystal structure.

2. Results and Discussion

2.1. Synthesis

Two synthetic pathways were followed. Path A is classic with the reaction of [Cu(H_2O)$_6$](AsF_6)$_2$ or a mixture of Cu(CH_3COO)$_2$ H_2O and (NH_4)$_2$CuCl$_4$ $2H_2O$, with NH_2trz in aqueous MeOH, leading to complexes **I** and **III**, respectively. Path B is more original. It requires first the synthesis of the formamidine **L·HCl** which was obtained by reacting NH_2trz with NaN_3 and HC(OEt)$_3$ in AcOH in an attempt to get the corresponding triazole-tetrazole molecule. The elemental analysis data suggest the resulting product to be a hydrochloride salt of a novel molecule (Scheme 1). Its ^{1}H NMR spectrum recorded in DMSO-d_6 contains two singlet signals at 8.65 and 8.83 ppm, corresponding to the formamidine and triazole CH protons, respectively.

Scheme 1. Synthesis of *N,N'*-bis-(1,2,4-triazole-4-yl)formamidine hydrochloride.
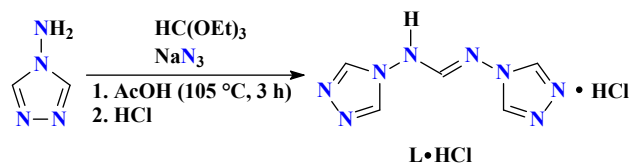
During our attempts to react Cu(II) salts with **L·HCl**, not surprisingly we noticed that this molecule was hydrolyzed in aqueous solution, and proves to be effective to slowly release NH_2trz and obtain crystals of Cu(II) complexes **II–IV**. It should be noted that the formulation of complex **IV** is rather unusual. In addition to the **L·HCl** hydrolysis, SiF_6^{2-} anions were identified. These anions area actually generated *in situ* by the reaction of BF_4^- anions (provided by the Cu(II) salt) with the glass of the H-tube used to grow crystals of the complex [21]. Furthermore, since **L·HCl** was introduced as a hydrochloride salt, complex **IV** contains Cl^- ions, which were provided by the ligand. This might be also true for **III** although $CuCl_2 \cdot 2H_2O$ was used as a source of Cu(II) ions.

## *2.2. IR and Diffuse Reflectance Spectroscopy*

IR spectra of **I–IV** each contain a band at about 1630 cm^{-1}, corresponding to the amide band of the NH_2 group (Figure S1). The spectra of **I** and **II** also exhibit an absorption band for the CuOH fragment at around 1000 cm^{-1}. There are also bands for the CH, NH_2 and H_2O groups in the range from 3000 to 3700 cm^{-1}. Additionally, the IR spectra of **I**, **II** and **IV** contain intense broad bands at about 740–800 cm^{-1}, arising from AsF_6^-, PF_6^- and SiF_6^{2-} anions, respectively (Figure S1). Diffuse reflectance -spectra of **I–IV** exhibit two broad bands in the range 400–900 nm corresponding to d-d transitions (Figure S2). A band from 200 to 400 nm has been attributed to the intraligand NH_2trz transitions. It should be noted that the IR and diffuse reflectance spectra of **I** and **II** are almost identical (Figures S1 and S2), testifying to isomorphous structures of these two complexes, as was also concluded from Xray diffraction (see next Section).

2.3. Structural Aspects

Recrystallization of **L·HCl** from an aqueous acetone solution leads to the formation of X-ray suitable crystals of **L**, which structure was initially solved and refined in the triclinic space group *P*1, and finally transformed to the monoclinic space group Cc. The molecular structure of **L** is shown in Figure 1. Table S1 in Supplementary Information contains the bond and angle values for **L**. The structure of **L** is stabilized by an intermolecular N–H···N hydrogen bonds between the NH hydrogen atom of the formamidine fragment and the triazole nitrogen atom of a neighboring molecule (Table S2 in Supplementary Information). As a result, the formation of 1D polymeric chains is observed in the structure of **L**.

Figure 1. Thermal ellipsoid (50%) plot of L along the *a*-axis. The nitrogen and carbon atoms are depicted in blue and grey, respectively. H-atoms were omitted for clarity.
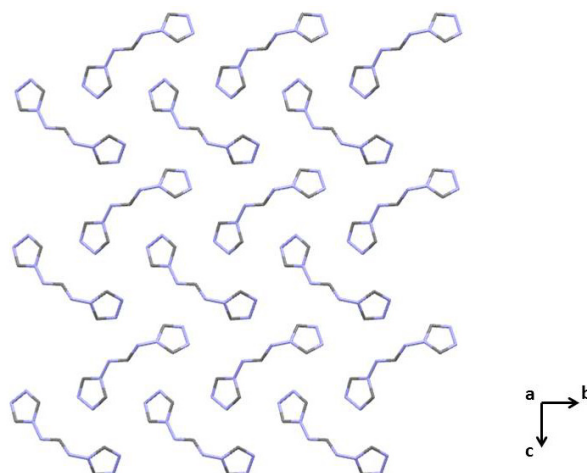
Complexes **I–IV** were obtained as X-ray suitable blue crystals by slow evaporation of a solvent from their solutions. It should be noted that several crystals of each complex have been checked by a single crystal X-ray analysis, indicating their full identity. Both complexes **I** and **II** crystallize in the tetragonal space group $I4_1/a$ and are isomorphous. Therefore, only the crystal structure of complex **II** will be described. Complexes **III** and **IV** crystallize in the monoclinic space group $P2_1/a$ and triclinic space group $P–1$, respectively, and each exhibit 1D cationic Cu(II) containing polymeric chains. The molecular structures of **II** and **III** are shown in Figure 2.

Figure 2. Thermal ellipsoid (50%) plot of **II** (**left**) and **III** (**right**). H-atoms and PF_6^- anions in **II**, and non-coordinated Cl^- anions and water molecules in **III** were omitted for clarity. The nitrogen atoms are depicted in blue, the carbon atoms in grey, the chloride ions in green and the copper atoms in red.
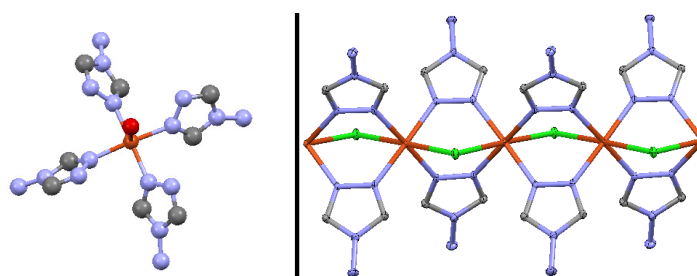

The discrete mononuclear complex **II** exhibits a distorted square pyramidal coordination polyhedron (Figure 2). In the basal plane, the Cu(II) atom is coordinated by four nitrogen atoms arising from four different NH$_2$trz ligands, while the apical position is occupied by a water oxygen atom (Figure 2). The Cu(II) atom in **II** is almost in the basal plane of the square pyramid and only slightly deviated above the plane (0.1890(4) Å). This is a surprising feature as in square pyramidal complexes the metal atom is usually located significantly above the basal plane [25]. This feature can be explained by the Cu···F interaction between the metal center and one of the fluorine atoms of the PF_6^- anion noted in **II**. Indeed, since the fluorine atom is located below the basal plane, it tends to drag the Cu(II) atom towards the bottom of the pyramid. The average Cu–N bond length is about 2.0 Å

(Table S3 in Supplementary Information). The Cu–O bond length is 2.263(3) Å. The N–Cu–N bond angles formed by the nitrogen atoms, corresponding to the NH_2trz ligands coordinated in a *cis*-arrangement are close to 90°, while the N–Cu–N bond angles formed by the nitrogen atoms in *trans*-position are about 170° (Table S3 in Supplementary Information). The N–Cu–O bond angles are about 95° (Table S3 in Supplementary Information).

Complexes **III** and **IV** each consist of 1D cationic Cu(II)-containing polymeric chains (Figures 2 and 3). The asymmetric unit of **IV** contains two non-equivalent Cu(II) atoms. Cu···Cu separations (~3.60–3.65 Å) in both complexes exceed the sum of van der Waals radii of Cu(II) which indicates the absence of any distinct intramolecular Cu···Cu interactions. Each metal center in **III** and **IV** is coordinated by two chlorine atoms in *trans*-configuration and by four nitrogen atoms arising from four different NH_2trz ligands (Figure 3). As a result, the formation of the distorted coordination octahedron is observed for both polymeric complexes. It should be highlighted that the structures of **III** and **IV** are unusual, with only one bridging μ_2-coordinated chloride ligand linking two neighboring Cu(II) atoms in a polymeric chain, because incorporation of chlorine into the coordination sphere of a transition metal in the triazole chains is known to result in triple bridges containing two μ_2-coordinated chloride ligands [4]. The latter situation is encountered in the crystal structure of $[Cu(Htrz)Cl_2]$ (Htrz = 4*H*-1,2,4-triazole) [26], which was the first one for a triazole complex elucidated by single crystal X-ray analysis, and in the related chain of $[Cu(\mu_2-NH_2trz)(\mu_2-Cl)_2]$ [10]. Thus, depending on the synthesis conditions, it is possible to obtain one or two μ_2-coordinated chloride ligands in the triple bridge, giving rise to charged or neutral chains, respectively.

Figure 3. Thermal ellipsoid (50%) plot of **III** along the *a* (**top**) and *c* axes (**bottom**). The nitrogen atoms are depicted in blue, the carbon atoms in grey, the chloride ions in green and the copper atoms in red. H-atoms were omitted for clarity.
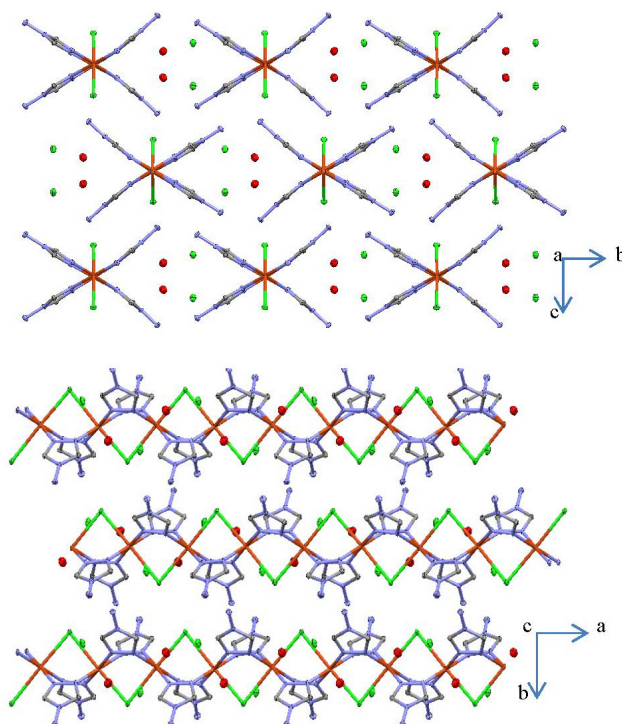
The Cu–N bond lengths in **III** and **IV** are similar to those found in the crystal structures of **I** and **II**, being about 2.0 Å (Tables S4 and S5 in Supplementary Information). The Cu–Cl bond lengths in **III** are about 2.69–2.78 Å (Table S4 in Supplementary Information), while the same bond lengths in **IV** are slightly shortened, about 2.65–2.72 Å (Table S5 in Supplementary Information). Thus, the equatorial positions on the octahedron are occupied by nitrogen atoms, while the chlorine atoms are in apical positions. Each coordinated Cl⁻ anion exhibits a bridging μ_2-coordination mode, while NH$_2$trz ligands exhibit a bridging bis-monodentate μ_2-N_1,N_2-coordination mode, linking two neighboring Cu(II) atoms (Figure 2). The N–Cu–N bond angles in each coordination octahedron of **III** and **IV**, formed by nitrogen atoms of the NH$_2$trz ligands coordinated in a *cis*-arrangement, are similar to those observed for **I** and **II** and are about 90°. The N–Cu–N bond angles formed by the nitrogen atoms in *trans*-position are significantly enlarged, 178–180° (Tables S4 and S5 in Supplementary Information). The N–Cu–Cl bond angles are in the range 85–95° both in **III** and **IV** (Tables S4 and S5 in Supplementary Information). The Cl–Cu–Cl bond angles are almost straight, 178–180°. The Cu–N–N bond angles defined by the Cu(II) atoms with NH$_2$trz ligands are 122–124°, while the Cu–Cl–Cu bond angles are about 84° in both polymeric complexes (Tables S4 and S5 in Supplementary Information). The Cu(II) atoms are located almost in the same plane with the triazole rings. There are two distinguishable octahedron orientations along the polymeric chains resulting in alternate *ababa...* order. Depending on the presence of intrachain ligand interactions, both *ababa...* [18,21,22] and *abcbab...* [27] order may be found in Cu(II) chains with triple μ_2-N_1,N_2-triazole bridges. In complexes, **III** and **IV**, the lack of direct intrachain ligand···ligand interactions, leads to the more regular *ababa...* order. It should be noted, that the angles between the planes formed by the triazole fragments coordinated to two Cu(II) atoms within a chain in **III** and **IV** are 74.23(13) and 66.55(12)°, respectively. This is considerably higher compared to Cu(II) μ_2-N_1,N_2-1,2,4-triazole chain complexes (e.g., 50.9(2)° for [Cu(μ_2-NH$_2$trz)$_3$]ZrF$_6$ H$_2$O [21]). The supramolecular aggregation in the structure of **II** consists of head-to-tail double sheets of mononuclear building units (Figure 4). Counter anions are located between double sheets, which are linked by a dense hydrogen bonding network involving amino groups of NH$_2$trz and the PF$_6^-$ anions (Table S2 in Supplementary Information). Each amine group is hydrogen bonded to two counter anions and one neighboring amine group. The hydrogen bonding between amine groups links mononuclear complexes of the same sheet (Figure 4). Each counter anion forms N–H···F hydrogen bonds with several mononuclear species, generating links between complexes of the same sheet and complexes corresponding to different double planes. Although the hydrogen atoms of coordinated H$_2$O were not located, interatomic distances between oxygen atoms of the water molecules of the sheet and the lone pair of the amine groups, corresponding to a further sheet of the same double plane, indicate the possible existence of hydrogen bonding between these ligands (predicted by the Mercury [28] software). Such hydrogen bonding was proposed by Yi *et al*. [24] to explain the double sheet structure.

Figure 4. Thermal ellipsoid (50%) plot of **II** along the *b* axis. The nitrogen atoms are depicted in blue, the carbon atoms in grey, the fluoride atoms in green, copper atoms in red and the phosphorus atoms in orange. H-atoms were omitted for clarity.
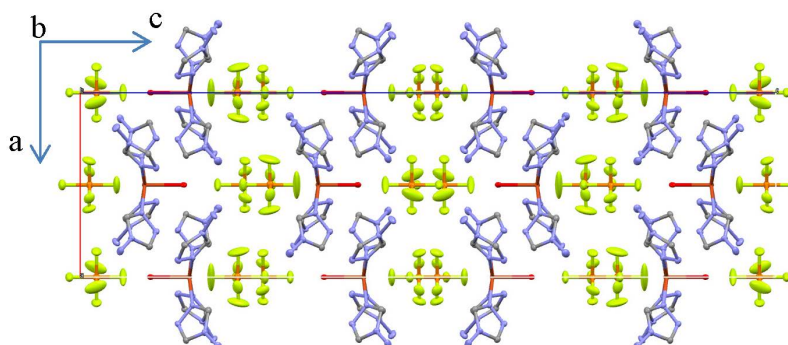
The crystal packing in **III** and **IV** is made of parallel Cu(II) chains, between which non-coordinated counter anions and water molecules are located (Figures 3 and 5). The Cu$\cdots$Cu distances in **III** are 3.6532(16) Å, while the same separations in **IV** are insignificantly shortened to 3.5994(16) and 3.6106(16) Å (Table 1), which was expected since no change of the first coordination sphere is noticed between **III** and **IV**. These values are about 0.08–0.14 Å longer than those for the similar Cu(II) chains, containing μ_2-*O* or μ_2-*N* bridging atoms, [11–13] but significantly shorter than the Cu$\cdots$Cu distances in the Cu(II) chains with three μ_2-1,2,4-triazole derivatives [27,29]. A shorter Cu$\cdots$Cu distance of 3.40 Å is found when only one μ_2-N_1,N_2-1,2,4-triazole is bridging as observed for [Cu(Htrz)Cl$_2$] [26]. The dihedral angles, formed by the μ_2-NH$_2$trz ligands linking two neighboring Cu(II) atoms, are about 5° and 12° in **III**. The former angle in **IV** is significantly reduced and of 0–2°, while the latter angle is very similar, 12–14°. These values are in a range characteristic for similar Cu(II) chains [12–14]. However, incorporation of the third μ_2-1,2,4-triazole derivative into the Cu(II) chain leads to a significant increase of the third dihedral angle, which might be explained by steric demands [27,29].

The presence of the amine groups, chloride ions and water molecules favors hydrogen bonding (Table S2 in Supplementary Information). Each chain is linked to a further two chains by the N–H$\cdots$Cl(coordinated) and N–H$\cdots$Cl(non-coordinated) $\cdots$H–N hydrogen bonding. Moreover, the N–H$\cdots$Cl$\cdots$H–O–H$\cdots$Cl$\cdots$H–N hydrogen bonds create connections to four neighboring chains. Thus, each chain is hydrogen bonded to six others in the structure of **III**. The crystal packing of **IV** consists of a dense hydrogen bonding network, which links neighboring chains (Table S2 in Supplementary Information). Parallel chains are linked by the multiples N–H$\cdots$Cl and N–H$\cdots$N hydrogen bonds. The N–H$\cdots$O–H$\cdots$F–Si–F$\cdots$H–N and N–H$\cdots$F–Si–F$\cdots$H–N hydrogen bonds connect the NH$_2$trz ligands throughout the whole network. Finally, rows of the SiF$_6^{2-}$ anions are bound by F$\cdots$H–O–H$\cdots$F hydrogen bonding. As a result of dense hydrogen bonding network is observed.

In **III**, voids between metal-containing chains are occupied by water-chloride $\{[Cl(H_2O)]^-\}_n$ supramolecular chains propagated by hydrogen bonds in a meander-like manner (Figure 6, Table S2 in Supplementary Information). These clusters are connected to cationic chains through hydrogen bonds formed between non-coordinated chloride ions and one of the NH$_2$ hydrogen atoms of the NH$_2$trz ligands (marked by red dash lines in Figure 6, Table S2 in Supplementary Information). Similar

structural arrangements of the water-chloride clusters, but in a pure zigzag manner, were observed for Co(II) and Pd(II) complexes [30,31].

Table 1. Overview of structural characteristics and magnetic data for 1D Cu(II) chains with 1,2,4-triazole ligands.

Complex	d(Cu$\cdots$Cu) (Å)	∠(Cu–N–N–Cu) [a] (°)	g	J (cm^{-1})	P (%)	$\chi_{TIP} \times 10^6$ (cm^3 mol^{-1})	zJ'/kB (cm^{-1})	Ref.
[Cu(μ_2-Htrz)(μ_2-Cl)$_2$]	3.405	−4.67	2.013	−12.4	-	-	-	[26,32]
[Cu(μ_2-NH$_2$trz)(μ_2-Cl)$_2$]	3.4895(5), 3.5210(5)	−5.8(3), 8.2(4)	2.26	−20.4	-	-	-	[10,32]
[Cu(μ_2-NH$_2$trz)$_2$Cl]Cl·H$_2$O (**III**)	3.653(2)	5.2(3), 11.7(2)	2.13	−128.4	0.65	390	11(5)	This work
[Cu(μ_2-NH$_2$trz)$_2$Cl](SiF$_6$)$_{0.5}$·1.5H$_2$O (**IV**)	3.599(2), 3.611(2)	−1.5(5), −13.9(4); −0.6(5), 11.5(4)	2.13, 2.13	−143.0, −139.9	1.02, 0.90	270, 350	80(4), 0	This work
[Cu(μ_2-NH$_2$trz)$_2$(μ_2-N$_3$-*N,N*)]NO$_3$	3.5035(8)	−7.8(4), −13.0(4)	2.22(1)	−17.7	-	-	-	[11]
[Cu(μ_2-NH$_2$trz)$_2$(μ_2-NCS-*N*)]ClO$_4$·0.5H$_2$O	3.470(2)	1.5(6), 2.0(5)	2.21	−51	-	-	-	[12]
[Cu(μ_2-NH$_2$trz)$_2$(μ_2-NO$_3$)]NO$_3$	3.5301(5)	−11.4(3), −13.8(3)	2.12	−75.1	-	-	−1.1	[11]
[Cu(μ_2-hyetrz)$_3$](ClO$_4$)$_2$·3H$_2$O [b]	3.829(2), 3.853(2)	−6.4(7), −10.7(9), −37.5(7); −3.0(7), −11.5(8), −38.0(6)	2.03(1)	−1.18(2)	-	-	-	[27]
[Cu(μ_2-hyetrz)$_3$](CF$_3$SO$_3$)$_2$·H$_2$O [b]	3.8842(4), 3.9354(4)	−3.3(2), −16.3(2), −28.98(19); −11.3(2), −13.8(2), −20.2(2)	2.20(1)	1.45(3)	-	-	-	[29]

[a] Dihedral angles must be compared by their magnitudes; [b] hyetrz = 4-(2'-hydroxyethyl)-1,2,4-triazole.

2.4. Magnetic Properties

Since no cooperative magnetism was expected for the mononuclear complexes **I** and **II**, magnetic properties were only investigated for polymeric complexes **III** and **IV**. Electron Paramagnetic Resonance (EPR) spectroscopy at X-band was used to determine the Lande *g*-factors that were thereafter used for a quantitative analysis of the magnetic properties. Room temperature X-band EPR spectra from powdered samples of **III** and **IV** are shown in Figure 7. The spectra consist of broad derivative-like signals with widths of ΔH_{pp} = 350 and 245 G for **III** and **IV**, respectively. Both complexes are characterized by a *g* value of 2.13.

Figure 5. Thermal ellipsoid (50%) plot of **IV** along the *a* (**top**) and *b* (**bottom**) axes. The nitrogen atoms are depicted in blue, the carbon atoms in grey, the fluoride atoms in light green, the chloride ions in green, the copper atoms in red, the silicium atoms in yellow and the oxygen atoms are depicted in red. H-atoms were omitted for clarity.
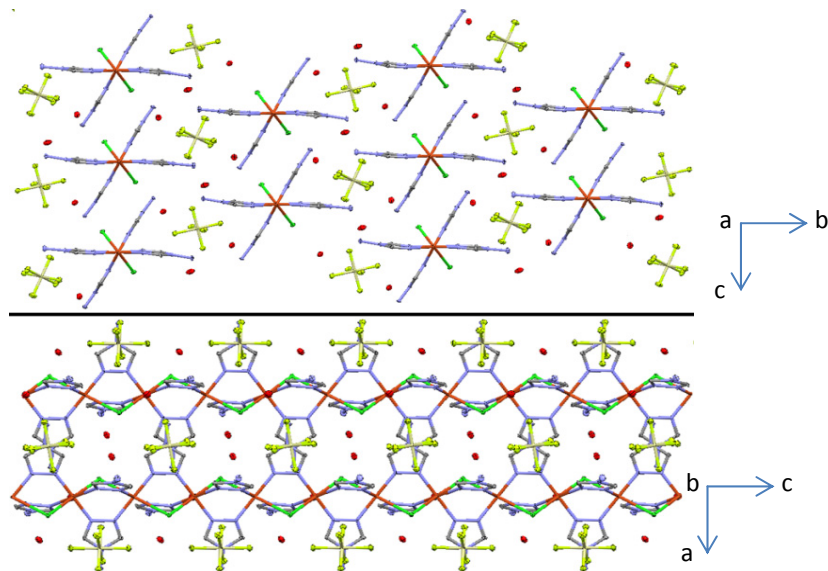
Figure 6. Thermal ellipsoid (50%) plot of the 1D polymeric chain formed by the $\{[Cl(H_2O)]^-\}_n$ cluster in the structure of **III**.
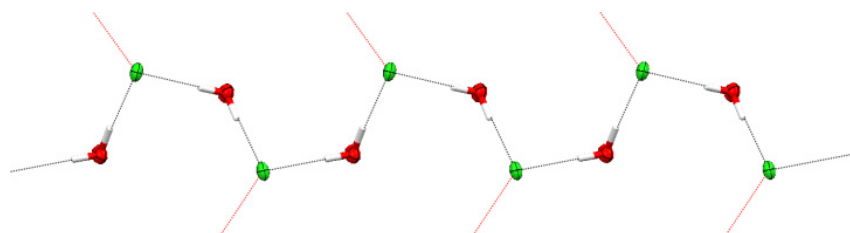

Figure 7. Room temperature X-band EPR spectra from powdered samples of **III** and **IV**.
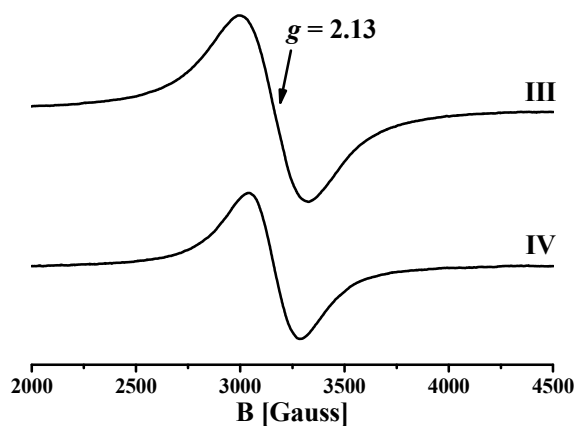
Magnetic susceptibility measurements were recorded for powdered samples of **III** and **IV** over the 5–300 K temperature range at an applied field of 0.1 T (Figure 8). At room temperature, the $\chi_M T$ values are 0.40 and 0.39 cm^3 mol^{-1} K for **III** and **IV**, respectively, comparable with that expected for one Cu(II) ion ($S = 1/2$). The temperature profiles of the magnetic susceptibility for both complexes are

very similar. As the temperature decreases, χ_M increases smoothly reaching a rather broad maximum at ca. 125 K for **III** and ca. 130 K for **IV**. Below these temperatures, χ_M decreases going through a minimum at ca. 25–30 K before increasing again abruptly (Figure 8).

Figure 8. Temperature dependence of molar susceptibility χ_M for powdered samples of **III** and **IV** at 0.1 T. Red solid lines are simulations based on the fitting procedure as discussed in the text. For **IV** the blue line corresponds to the fit obtained assuming $zJ' = 0$.
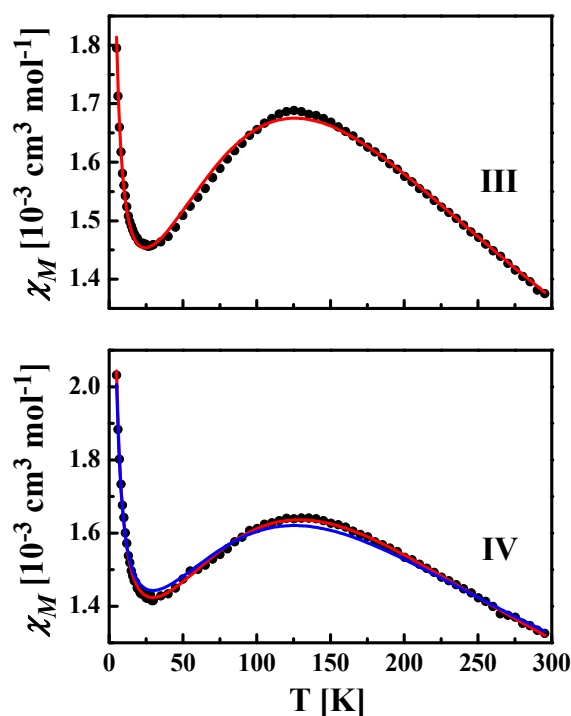
On the basis of the crystal structures of **III** and **IV**, the magnetic behavior of both complexes was approximated assuming a 1D antiferromagnetic (AF) chain governed by the exchange coupling Hamiltonian: $H = -J\Sigma S_i S_{i+1}$, where J is the isotropic interaction parameter. The temperature dependence of the magnetic susceptibility for such a 1D system is adequately described by the Bonner-Fischer approximation [33]:

$$\chi_M = \frac{N\beta^2 g^2}{k_B T}\left(\frac{0.25 + 0.074975x + 0.075235x^2}{1 + 0.9931x + 0.172135x^2 + 0.757825x^3}\right) \tag{1}$$

with $x = |J|/k_B T$ and the other terms having their usual meanings.

Since the crystal packing for these 1D chains reveals several inter-chain interactions (Figures 3 and 5), a mean field correction was considered using a corrected susceptibility χ_{cor}, where zJ' corresponds to the interchain interaction parameter [34]:

$$\chi_{cor} = \frac{\chi_M}{1 - \frac{zJ'\chi_M}{Ng^2\beta^2}} \tag{2}$$

The increase of χ_M below 30 K is attributed to paramagnetic monomeric impurities and/or short chains after chain breaking [35,36] with $S = 1/2$, for which the magnetic susceptibility, χ_{IMP}, follows

the Curie law. Overall, the susceptibility data were best fitted following the equation: $\chi_M = (1 - \rho)\chi_{cor} + \rho\chi_{IMP} + \chi_{TIP}$, where ρ is the fraction of paramagnetic impurities and χ_{TIP} is the temperature independent paramagnetism (TIP). The parameters obtained from these simulations are listed in Table 1, considering two situations for **IV**, with or without intermolecular interactions, the second situation being the less favorable according to fitting results (Figure 8).

Despite the similar nature of the [Cu(μ_2-NH$_2$trz)$_2$Cl] polymeric unit in **III** and **IV**, the latter exhibits stronger inter-chain magnetic interactions zJ' (Table 1). The strong AF intra-dimer coupling J determined in **III** and **IV** is much higher than those of previously reported 1D Cu(II) complexes made of two μ_2-N_1,N_2-NH$_2$trz and another bridging atom, *i.e.*, N in [Cu(μ_2-NH$_2$trz)$_2$(μ_2-N$_3$-N,N)]NO$_3$ [11], or [Cu(μ_2-NH$_2$trz)$_2$(μ_2-NCS-N)]ClO$_4$·0.5H$_2$O [12], and O in [Cu(μ_2-NH$_2$trz)$_2$(μ_2-NO$_3$)]NO$_3$ (Table 1) [13]. These results allow us to evidence an intermediate case between two structural situations by disclosing the crystal structures of the chain compounds **III** and **IV** which show a new bridge type of formula [Cu(NH$_2$trz)$_2$Cl]$^+$. Interestingly, this configuration reveals higher intra-dimer coupling constants compared to the initial case where Cu(II) chains, of formula [Cu(Rtrz)$_3$]$^{2+}$, made of three Rtrz bridges show very weak $|J|$ values [27,29], and the third case where neutral Cu(II) chains [Cu(NH$_2$trz)Cl$_2$], show weak J values [10,32]. Despite the high J values of **III** and **IV**, the record ones reported so far for this substance class are hold by Drabent *et al*. for [Cu(μ_2-OH)(μ_2–XPhtrz)]BF$_4$·H$_2$O and [Cu(μ_2-OH) (μ_2-XPhtrz)(H$_2$O)]NO$_3$ (X = Cl, Br; XPhtrz = *N*-[(*E*)-(4-*R*-methylidene]-4*H*-1,2,4-triazol-4-amine) which range from −391(3) to −608(2) cm^{-1} [35]. Ab initio calculations would be useful to appreciate the origin of the magnitude of the coupling constants in these model Cu(II) chain compounds.

3. Experimental Section

3.1. General Procedures

Infrared spectra (KBr) were recorded with a FTIR-8400S SHIMADZU spectrophotometer (Shimadzu, Kyoto, Japan) in the range 400–3600 cm^{-1}. ^{1}H NMR spectra in DMSO-d_6 were obtained on a Bruker Avance 300 MHz spectrometer (Billerica, MA, USA) at 25 °C. Chemical shifts are reported with reference to SiMe$_4$. Diffuse reflectance spectra were obtained with a Varian Cary 5E spectrometer (Palo Alto, CA, USA) using polytetrafluoroethylene (PTFE) as a reference. Elemental analyses were performed at University College London, UK. Magnetic susceptibility measurements were performed on a MPMS-5500 Quantum Design instrument (San Diego, CA, USA) in the temperature range 5–300 K. Experimental data were corrected for the sample holder and for the diamagnetic contribution of the sample using Pascal's constants. X-band EPR spectra at room temperature were recorded on a Bruker ER 200D-SRC X-band spectrometer (Billerica, MA, USA) equipped with an NMR Gaussmeter, and an Anritsu microwave frequency counter. The following conditions were applied: microwave power 59 mW, modulation amplitude 25 Gpp, microwave frequency 9.42 GHz.

3.2. Syntheses

***N*,*N'*-bis-(1,2,4-triazole-4-yl)formamidine hydrochloride** (**L·HCl**): A solution of NH$_2$trz (4.9 g, 58.3 mmol), HC(OEt)$_3$ (9.8 g, 66.1 mmol) and NaN$_3$ (3.9 g, 60 mmol) in AcOH (25 mL) was heated at

105 °C for 3 h. The reaction mixture was then cooled and 37% aqueous HCl (5.8 g, 58.3 mmol) was added. The resulting solution was filtered and concentrated under reduced pressure to give a yellowish solid, which was washed by hot EtOH (80 mL) to afford a white solid. Yield: 1.5 g (12%). mp > 200 °C. IR: v = 3105 (*m*), 3095 (*m*), 3068 (*m*), 3025 (*w*), 2971 (*vw*), 1657 (*s*), 1491 (*m*), 1447 (*w*), 1393 (*m*), 1362 (*w*), 1318 (*m*), 1285 (*m*), 1264 (*m*), 1173 (*m*), 1055 (*s*), 990 (*m*), 959 (*m*), 947 (*m*), 899 (*w*), 872 (*m*), 833 (*m*), 764 (*m*), 614 (*s*), 532 (*w*) cm^{-1}. ^{1}H NMR: δ = 8.65 (s, 1H, CH), 8.83 (s, 4H, CH, 1,2,4-triazole) ppm. Anal. Calc. for $C_5H_7ClN_8$ (214.62): C 27.98, H 3.29, N 52.21. Found: C 27.63, H 2.99, N 51.11. Crystals of **L** suitable for a single crystal X-ray analysis were obtained by dissolving 0.2 g of **L·HCl** in H_2O–acetone (5 mL; 50:50, *v/v*) solution, which was slowly evaporated at room temperature affording single crystal on standing (4 days).

[Cu(NH$_2$trz)$_4$(H$_2$O)](AsF$_6$)$_2$ (I): A solution of NH$_2$trz (0.252 g, 3 mmol) in MeOH (10 mL) was added drop wise to a solution of [Cu(H$_2$O)$_6$](AsF$_6$)$_2$ (0.550 g, 1 mmol) in MeOH (5 mL). The resulting blue precipitate was filtered off, washed with MeOH and dried in a desiccator. A small amount of a solid material (0.050 g) was dissolved in water (100 mL). Crystals suitable for a single crystal X-ray analysis were obtained on standing (12 months) with slow evaporation of the solvent. Yield: 0.376 g (63%). Anal. Calc. for $C_8H_{18}As_2CuF_{12}N_{16}O$ (795.71): C 12.08, H 2.28, N 28.16. Found: C 12.17, H 2.23, N 28.24.

[Cu(NH$_2$trz)$_4$(H$_2$O)](PF$_6$)$_2$ (II): **L·HCl** (0.300 g, 1.39 mmol) was dissolved in water (10 mL). Then a solution of KPF$_6$ (0.208 g, 1.13 mmol) and CuCl$_2$·2H$_2$O (0.097 g, 0.57 mmol) in water (10 mL) was added dropwise leading to a precipitate. To the resulting mixture, additional water (500 mL) was added and the solution was heated until the precipitate completely dissolved. Crystals suitable for a single crystal X-ray analysis were obtained on standing (8 months) with slow evaporation of the solvent and slow delivery of NH$_2$trz by hydrolysis of **L**. Yield: 0.285 g (74%). Anal. Calc. for $C_8H_{18}CuF_{12}N_{16}OP_2$ (707.8): C 13.57, H 2.56, N 31.64. Found: C 14.37, H 2.52, N 33.30.

[Cu(μ$_2$-NH$_2$trz)$_2$Cl]Cl·H$_2$O (III): Path A: A solution of Cu(CH$_3$COO)$_2$·H$_2$O (0.106 g, 0.053 mmol) in water (5 mL) was added to a solution of (NH$_4$)$_2$CuCl$_4$·2H$_2$O (0.147 g, 0.053 mmol) in the same solvent (5 mL). The resulting blue solution was added to a solution of NH$_2$trz (0.134 g, 0.159 mmol) in MeOH (5 mL). Then the mixture was cooled in ice till the blue solid was precipitated. The obtained solid material was filtered off and dissolved in water (50 mL) upon heating. Crystals suitable for a single crystal X-ray analysis were obtained on standing (several weeks) after slow evaporation of the solvent. Yield: 0.114 g. Path B: **L·HCl** (0.300 g, 1.39 mmol) was dissolved in water (10 mL). Then a solution of CuCl$_2$·2H$_2$O (0.097 g, 0.57 mmol) in water (10 mL) was added dropwise leading to the formation of a precipitate. To the resulting mixture, additional water (450 mL) was added and the solution was heated until the precipitate completely dissolved. Crystals suitable for a single crystal X-ray analysis were obtained on standing (6 months) after slow evaporation of the solvent and slow delivery of NH$_2$trz by hydrolysis of **L**. Yield: 0.128 g (75%). Anal. Calc. for $C_4H_{10}Cl_2CuN_8O$ (320.63): C 14.98, H 3.14, N 34.95. Found: C 15.11, H 3.19, N 34.82.

[Cu(μ$_2$-NH$_2$trz)$_2$Cl](SiF$_6$)$_{0.5}$·1.5H$_2$O (IV): **L·HCl** (0.300 g, 1.39 mmol) was dissolved in water (6 mL) and inserted in the left arm of a H-tube. A 50% wt. aqueous solution of Cu(BF$_4$)$_2$ (260 μL, 0.55 mmol) was placed in the right arm of a H-tube. Then the tube was carefully filled with water and

sealed to prevent evaporation of the solvent. Crystals suitable for a single crystal X-ray analysis were obtained on standing (5 months) after slow delivery of NH$_2$trz by hydrolysis of **L** and formation of SiF$_6^{2-}$ by the reaction of BF$_4^-$ with the glass tube. Yield: 0.137 g (34%). Anal. Calc. for C$_8$H$_{22}$Cl$_2$Cu$_2$F$_6$N$_{16}$O$_3$Si (730.44): C 13.15, H 3.04, N 30.68. Found: C 13.28, H 2.97, N 30.53.

3.3. X-ray Crystallography

The X-ray intensity data were collected with a MAR345 image plate (Norderstedt, Germany) using Mo-K$_\alpha$ ($\lambda = 0.71069$ Å) radiation. The crystal was chosen, mounted in inert oil and transferred quickly to the cold gas stream for flash cooling. Crystal data and data collection parameters are summarized hereafter. The unit cell parameters were refined using all the collected spots after the integration process. The data were not corrected for absorption (for **L**, **III**, **IV**), but the data collection mode partially takes the absorption phenomena into account. The structures were solved by direct methods with SHELXS [37]. The structure was refined by full-matrix least-squares on F^2 using SHELXL [37]. All non-hydrogen atoms were refined with anisotropic temperature factors. All hydrogen atoms were placed on calculated positions with temperature factors 1.2 times higher than their parent atoms (1.5 for methyl and OH hydrogens). The Fourier density map for **II** reveals a high residual peak next to the copper coordinated oxygen atom. Inspection of the native Patterson map reveals a large off origin peak (peak height > 50% orgin peak) positioned at 0.5 0 0.25, which is believed to indicate translational disorder. Applying the translation to the Cu atom situated on the 2-fold axis this gives a peak at 0.0000 0.7500 0.0901 or 0.5000 0.2500 0.5901 (+1/2 +1/2 +1/2) (given the **I** centering), which is also the position of the high residual peak in the Fourier map. The crystals (in total three full datasets were measured all giving the same outcome) have all some degree of non-crystallographic translational symmetry and thus consists of two domains which are translated by 1/2 in the *z*-direction. Figures were generated using the Mercury software [14].

Crystal data for L: C$_5$H$_6$N$_8$, M_r = 178.18 g mol^{-1}, Monoclinic, space group *Cc*, *a* = 3.7400(7), *b* = 21.081(4), *c* = 9.2000(18) Å, β = 100.00(3)°, *V* = 714.3(2) Å^3, *Z* = 4, ρ = 1.657 g cm^{-3}, *T* = 293(2) K, μ(Mo-Kα) = 0.122 mm^{-1}, reflections: 3630 collected, 1345 unique, R_{int} = 0.0466, R_1(all) = 0.0399, wR_2(all) = 0.0958.

Crystal data for II: C$_8$H$_{16}$CuF$_{12}$N$_{16}$OP$_2$, M_r = 705.85 g mol^{-1}, tetragonal, space group *I*4$_1$/*a*, *a* = *b* = 10.7557(1), *c* = 40.574(1) Å, *V* = 4693.8(1) Å^3, *Z* = 8, ρ = 1.998 g cm^{-3}, *T* = 100(2) K, μ(Mo-Kα) = 1.204 mm^{-1}, reflections: 23,890 collected, 2243 unique, R_{int} = 0.046, R_1(all) = 0.0758, wR_2(all) = 0.201.

Crystal data for III: C$_4$H$_{10}$Cl$_2$CuN$_8$O, M_r = 320.65 g mol^{-1}, monoclinic, space group *P*2$_1$/*a*, *a* = 7.303(3), *b* = 13.838(5), *c* = 11.019(4) Å, β = 101.67(2)°, *V* = 1090.6(7) Å^3, *Z* = 4, ρ = 1.953 g cm^{-3}, *T* = 101(2) K, μ(Mo-Kα) = 2.486 mm^{-1}, reflections: 28,160 collected, 2225 unique, R_{int} = 0.055, R_1(all) = 0.0316, wR_2(all) = 0.0915.

Crystal data for IV: C$_8$H$_{22}$Cl$_2$Cu$_2$F$_6$N$_{16}$O$_3$Si, M_r = 730.51 g mol^{-1}, triclinic, space group *P*–1, *a* = 7.210(3), *b* = 11.673(4), *c* = 15.271(5) Å, α = 70.35(2), β = 82.16(2), γ = 79.55(2)°, *V* = 1186.4(8) Å^3, *Z* = 2, ρ = 2.045 g cm^{-3}, *T* = 105(2) K, μ(Mo-Kα) = 2.167 mm^{-1}, reflections: 19,683 collected, 4296 unique, R_{int} = 0.066, R_1(all) = 0.0504, wR_2(all) = 0.1124.

CCDC 902803 (**L**), 902805 (**II**), 902804 (**III**) and 902806 (**IV**) contain the supplementary crystallographic data. These data can be obtained free of charge via http://www.ccdc.cam.ac.uk/conts/retrieving.html, or from the Cambridge Crystallographic Data Centre, 12 Union Road, Cambridge CB2 1EZ, UK; Fax: (+44) 1223-336-033; or E-Mail: deposit@ccdc.cam.ac.uk.

4. Conclusions

In this work, two Cu(II) NH$_2$trz mononuclear complexes **I** and **II** have been isolated and structurally characterized, which is rather uncommon for a ligand routinely used in coordination chemistry to afford polynuclear complexes. Our work opens interesting perspectives because such materials are described as potential energy sources for ballistic applications [23,38,39]. We have also presented two novel examples of 1D NH$_2$trz chains, **III** and **IV**, where neighboring Cu(II) atoms are linked by two bridging bis-monodentate μ_2-N_1,N_2-NH$_2$trz and one bridging μ_2-chloride ligand, a configuration which was not yet explored for this family of coordination polymers. Their resulting strong antiferromagnetic coupling has been quantitatively evaluated after considering precise SQUID and EPR measurements.

Conflicts of Interest

The authors declare no conflict of interest.

References

1. Saini, M.S.; Dwivedi, J. Synthesis and biological significances of 1,2,4-triazole and its derivatives: A review. *Int. J. Pharm. Sci. Res.* **2013**, *4*, 2866–2879.
2. Tamura, K.; Inoue, K.; Takahashi, M.; Matsuo, S.; Irie, K.; Kodama, Y.; Ozawa, S.; Nishikawa, A.; Yoshida, M. Dose-response involment of constitutive androstate receptor in mouse liver hypertrophy induced by triazole fungicides. *Toxicol. Lett.* **2013**, *221*, 47–56.
3. Zhang, J.-P.; Zhang, Y.-B.; Lin, J.-B.; Chen, X.-M. Metal azolate frameworks: From crystal engineering to functional materials. *Chem. Rev.* **2012**, *112*, 1001–1033.
4. Haasnoot, J.G. Mononuclear, oligonuclear and polynuclear metal coordination compounds with 1,2,4-triazole derivatives as ligands. *Coord. Chem. Rev.* **2000**, *200–202*, 131–185.
5. Naik, A.D.; Dîrtu, M.M.; Railliet, A.P.; Marchand-Brynaert, J.; Garcia, Y. Coordination polymers and metal organic frameworks derived from 1,2,4-triazole amino acid linkers. *Polymers* **2011**, *3*, 1750–1775.

6. Wu, X.-Y.; Kuang, X.-F.; Zhao, Z.-G.; Chen, S.-C.; Xie, Y.-M.; Yu, R.-M.; Lu, C.-Z. A series of POM-based hybrid materials with different copper/aminotriazole motif. *Inorg. Chim. Acta* **2010**, *363*, 1236–1242.

7. Zhou, J.-H.; Cheng, R.-M.; Song, Y.; Li, Y.-Z.; Yu, Z.; Chen, X.-T.; Xue, Z.-L.; You, X.-Z. Syntheses, structures, and magnetic properties of unusual nonlinear polynuclear copper(II) complexes containing derivatives of 1,2,4-triazole and pivalate ligands. *Inorg. Chem.* **2005**, *44*, 8011–8022.

8. Yang, E.-C.; Ding, B.; Liu, Z.-Y.; Yang, Y.-L.; Zhao, X.-J. Structural transformation from a discrete $Cu(II)_4$ cluster to two extended $Cu(II)_4$ + $Cu(II)_1$ chain-based three-dimensional frameworks by changing the spacer functionality: Synthesis, crystal structures, and magnetic properties. *Cryst. Growth Des.* **2012**, *12*, 1185–1192.

9. Yang, E.-C.; Liu, Z.-Y.; Zhang, C.-H.; Yang, Y.-L.; Zhao, X.-J. Structural diversity directed by switchable coordination of substitute groups in a ternary Cu(II)-triazole-sulfoisophthalate self-assembly system: Synthesis, crystal structures and magnetic behavior. *Dalton Trans.* **2013**, *42*, 1581–1590.

10. Romanenko, G.V.; Savelieva, Z.A.; Podberezskaya, N.V.; Larionov, S.V. Structure of the Cu(II) chloride complex with 4-amino-l,2,4-triazole $CuC_2H_4N_4Cl_2$. *J. Struct. Chem.* **1997**, *38*, 171–176.

11. Liu, J.C.; Fu, D.G.; Zhuang, J.Z.; Duan, C.Y.; You, X.Z. Linear trinuclear and one-dimensional copper(II) complexes containing co-bridging end-on azido and triazole ligands. Crystal structures and magnetic properties of $[Cu_3(atrz)_2(N_3)_6]$ and $[Cu(atrz)_2(N_3)]NO_3$ (atrz = 4-amino-1,2,4-triazole). *J. Chem. Soc.-Dalton Trans.* **1999**, *14*, 2337–2342.

12. Ding, B.; Huang, Y.Q.; Liu, Y.Y.; Shi, W.; Cheng, P. Synthesis, structure and magnetic properties of a novel 1D coordination polymer $\{[Cu_2(amtrz)_4(1,1-\mu-NCS)_2](ClO_4)_2 \cdot H_2O\}_n$ *Inorg. Chem. Commun.* **2007**, *10*, 7–10.

13. Mahenthirarajah, T.; Li, Y.; Lightfoot, P. Organic-inorganic hybrid chains and layers constructed from copper-amine cations and early transition metal (Nb, Mo) oxyfluoride anions. *Dalton Trans.* **2009**, *17*, 3280–3285.

14. García-Couceiro, U.; Castillo, O.; Luque, A.; García-Terán, J.P.; Beobide, G.; Román, P. One-dimensional oxalato-bridged metal(II) complexes with 4-amino-1,2,4-triazole as apical ligand. *Eur. J. Inorg. Chem.* **2005**, doi:10.1002/ejic.200500332.

15. Yang, E.-C.; Liu, Z.-Y.; Zhao, L.-N.; Yang, Y.-L.; Zhang, C.-H.; Zhao, X.-J. Ligand-deprotonation induced structural diversity in a ternary Cu(II)-triazole-tetracarboxylate self-assembly system: Synthesis, crystal structures, and magnetic behavior. *CrystEngComm* **2011**, *13*, 5401–5408.

16. Liu, Z.-Y.; Su, Y.-H.; Yang, E.-C.; Zhao, X.-J. Structural transformation from a coplanar layer to a linear chain by switchable coordination of exocyclic amino group. *Inorg. Chem. Commun.* **2012**, *26*, 56–59.

17. Qiao, L.-Y.; Zhang, J.; Li, Z.-J.; Qin, Y.-Y.; Yin, P.-X.; Cheng, J.-K.; Yao, Y.-G. Hydrogen-bond directed self-assembly of a novel 2D → 3D polythreading with finite components based on rigid ligand. *J. Mol. Struct.* **2011**, *994*, 1–5.

18. Dîrtu, M.M.; Neuhausen, C.; Naik, A.D.; Rotaru, A.; Spinu, L.; Garcia, Y. Insights into the origin of cooperative effects in the spin transition of $[Fe(NH_2trz)_3](NO_3)_2$: The role of supramolecular

interactions evidenced in the crystal structure of [Cu(NH$_2$trz)$_3$](NO$_3$)$_2$ H$_2$O. *Inorg. Chem.* **2010**, *49*, 5723–5736.

19. Garcia, Y.; Campbell, S.J.; Lord, J.S.; Boland, Y.; Ksenofontov, V.; Gutlich, P. Dynamics and supramolecular organization of the 1D spin transition polymeric chain compound [Fe(NH$_2$trz)$_3$](NO$_3$)$_2$. Muon spin relaxation. *J. Phys. Chem. B* **2007**, *111*, 11111–11119.

20. Grosjean, A.; Daro, N.; Kauffmann, B.; Kaiba, A.; Letard, J.-F.; Guionneau, P. The 1-D polymeric structure of the Fe(NH$_2$trz)$_3$(NO$_3$)$_2$·nH$_2$O (with *n* = 2) spin crossover compound proven by single crystal investigations. *Chem. Commun.* **2011**, *47*, 12382–13284.

21. Drabent, K.; Ciunik, Z. Counter anion dependent symmetry of Cu(II)-4-amino-1,2,4-triazole polymeric chains. *Chem. Commun.* **2001**, *14*, 1254–1255.

22. Dîrtu, M.M.; Rotaru, A.; Gillard, D.; Linares, J.; Codjovi, E.; Tinant, B.; Garcia, Y. Prediction of the spin transition temperature in Fe(II) one-dimensional coordination polymers: An anion based database. *Inorg. Chem.* **2009**, *48*, 7838–7852.

23. Sinditskii, V.P.; Sokol, V.I.; Fogelzang, A.E.; Dutov, M.D.; Serushkin, V.V.; Poraikoshits, M.A.; Svetlov, B.S. The vibrational Spectra and structure of coordination compounds of metals with 4-amino-1,2,4-triazole as bidendate ligand. *Russ. J. Inorg. Chem.* **1987**, *32*, 1950.

24. Yi, L.; Du, J.-Y.; Liu, S.; Wang, X.-X. Supramolecular polymers of two novel 4-substituted-1,2,4-triazolate complexes: [Cd(^{p}Cltrz)$_2$(NCS)$_2$(H$_2$O)$_2$] and [Cu(4-atrz)$_4$(Cl)$_{0.5}$(H$_2$O)$_{0.5}$](ClO$_4$)$_{1.5}$ (^{p}Cltrz: 4-(p-chlorophenyl)-1,2,4-triazole; 4-atrz: 4-amino-1,2,4-triazole). *J. Chem. Res.* **2004**, *1*, 29–31.

25. Huheey, J.; Keiter, E.; Keiter, E.A.; Richard, L. *Inorganic Chemistry: Principles of Structure and Reactivity*; HarperCollins College: New York, NY, USA, 1993.

26. Jarvis, J. The crystal structure of a complex of cupric chloride and 1:2:4-triazole. *Acta Cryst.* **1962**, *15*, 964–966.

27. Garcia, Y.; van Koningsbruggen, P.J.; Bravic, G.; Guionneau, P.; Chasseau, D.; Cascarano, G.L.; Moscovici, J.; Lambert, K.; Michalowicz, A.; Kahn, O. Synthesis, crystal structure, EXAFS, and magnetic properties of catena-poly µ-tris(4-(2-hydroxyethyl)-1,2,4-triazole-N_1,N_2)copper(II) diperchlorate trihydrate: Relevance with the structure of the iron(II) 1,2,4-triazole spin transition molecular materials. *Inorg. Chem.* **1997**, *36*, 6357–6365.

28. Macrae, C.F.; Bruno, I.J.; Chisholm, J.A.; Edgington, P.R.; McCabe, P.; Pidcock, E.; Rodriguez-Monge, L.; Taylor, R.; van de Streek, J.; Wood, P.A. Mercury CSD 2.0—New features for the visualization and investigation of crystal structures. *J. Appl. Cryst.* **2008**, *41*, 466–470.

29. Garcia, Y.; van Koningsbruggen, P.J.; Bravic, G.; Chasseau, D.; Kahn, O. A Cu(II) chain compound showing a ferromagnetic coupling through triple N_1,N_2-1,2,4-triazole bridges. *Eur. J. Inorg. Chem.* **2003**, *2*, 356–362.

30. Saha, M.K.; Bernal, I. Environment-controlled switching between cyclic hexamer and helical conformations of a water chloride cluster: An old compound viewed in a new perspective. *Inorg. Chem. Commun.* **2005**, *8*, 871–873.

31. Bai, S.-Q.; Quek, G.Y.H.; Koh, L.L.; Andy Hor, T.S. Crystallographic analysis of different water-halide cluster blends in cationic [(SNS)Pd(II)] pincer complexes. *CrystEngComm* **2010**, *12*, 226–233.

32. Emori, S.; Inoue, M.; Kubo, M. Magnetic susceptibilities and broad-line pmr spectra of dichloro(pyridazine)copper(II) and related compounds. *Bull. Chem. Soc. Jpn.* **1972**, *45*, 2259–2265.

33. Bonner, J.C.; Fisher, M.E. Linear magnetic chains with anisotropic coupling. *Phys. Rev. A* **1964**, *135*, 640–658.

34. Estes, W.E.; Gavel, D.P.; Hatfield, W.E.; Hodgson, D.J. Magnetic and structural characterization of dibromo- and dichlorobis(thiazole)copper(II). *Inorg. Chem.* **1978**, *17*, 1415–1421.

35. Drabent, K.; Ciunik, Z.; Ozarowski, A. X-ray crystal structures, electron paramagnetic resonance, and magnetic studies on strongly antiferromagnetically coupled mixed μ-hydroxide-μ-N_1,N_2-triazole-bridged one dimensional linear chain copper(II) complexes. *Inorg. Chem.* **2008**, *47*, 3358–3365.

36. Kachi-Terajima, C.; Ishii, M.; Saito, T.; Kanadani, C.; Harada, T.; Kuroda, R. Homochiral 1D helical chain based on an achiral Cu(II) complex. *Inorg. Chem.* **2012**, *51*, 7502–7507.

37. Sheldrick, G.M. A short history of SHELX. *Acta Cryst. A* **2008**, *64*, 112–122.

38. Cudziło, S.; Trzciński, W.; Nita, M.; Michalik, S.; Krompiec, S.; Kruszyński, R.; Kusz, J. Preparation, crystal structure and explosive properties of copper(II) perchlorate complex with 4-amino-1,2,4-triazole and water. *Propellants Explos. Pyrotech.* **2011**, *36*, 151–159.

39. Talawar, M.B.; Divekar, C.N.; Makashir, P.S.; Asthana, S.N. Tetrakis-(4-amino-1,2,4-triazole) copper perchlorate: A novel ballistic modifier for composite propellants. *J. Propuls. Power* **2005**, *21*, 186–189.